

DIAMOND-II STORAGE RING DEVELOPMENTS AND PERFORMANCE STUDIES

I.P.S. Martin, H.-C. Chao, R.T. Fielder, H. Ghasem, J. Kallestrup, T. Olsson, B. Singh, S. Wang,
 Diamond Light Source, Oxfordshire, U.K.

Abstract

The Diamond-II project includes a replacement of the existing double-bend achromat storage ring with a modified hybrid 6-bend achromat, doubling the number of straight sections and increasing the photon beam brightness by up to two orders of magnitude. The design and performance characterisation of the new storage ring has continued to progress, including a switch to an aperture-sharing injection scheme, freezing the magnet layout, studying the impact of IDs, developing a commissioning procedure and investigating collective effects. In this paper we present an overview of these studies, including final performance estimates.

INTRODUCTION

The lattice design for the Diamond-II storage ring remains largely unchanged since the work presented in [1], with the majority of effort focussed on developing the engineering design and characterising the performance of the lattice under realistic conditions [2]. This paper presents an overview of these studies. For reference, a plot of the Twiss parameters for a single cell spanning long, mid and standard straights is shown in Fig. 1 and a summary of the main lattice parameters for the nominal optics is given in Table 1.

DIAMOND-II STORAGE RING

Lattice Modifications

Although the magnet layout and nominal optics remains unchanged, minor modifications have been made to accommodate the evolving engineering design. The largest change has occurred on the mid-to-long straight (ML) and mid-to-standard straight (MS) girders where the dispersion and beta-functions are large, with a total of three collimators in each plane. Optimal gaps of ± 3.5 mm horizontally and ± 1.5 mm vertically were arrived at after an extensive investigation into the collection efficiency and the impact on lifetime and injection. Details of these studies can be found in [3].

A review of the magnet strength limits has been conducted, the purpose of which was to ensure there is sufficient tuning range to allow for future changes to the machine optics and nonlinear optimisation. These studies included:

A review of the magnet strength limits has been conducted, the purpose of which was to ensure there is sufficient tuning range to allow for future changes to the machine optics and nonlinear optimisation. These studies included:

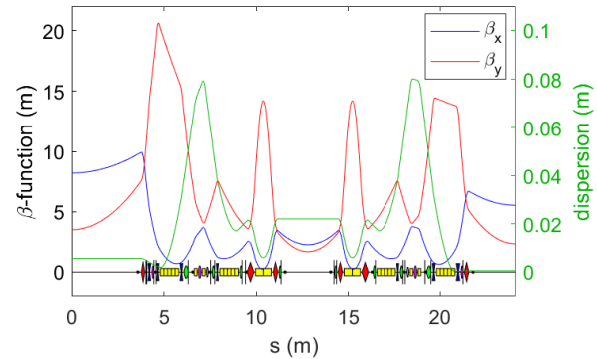


Figure 1: Twiss parameters for one M-H6BA cell including long, mid and standard straight sections.

Table 1: Summary of Diamond-II Lattice Parameters

Parameter	Bare Lattice	
Circumference (m)	561.561	
Tot. Bending Angle (deg)	388.8	
Betatron Tunes	[54.15, 20.27]	
Nat. Chromaticity	[-67.6, -88.5]	
Mom. Comp. Factor	1.04×10^{-4}	
Parameter	Bare Lattice	IDs Closed
Nat. Emittance (pm.rad)	161.7	121.0
Nat. En. Spread (%)	0.094	0.110
RF Voltage (MV)	1.4	2.5
Nat. Bunch Length (ps)	12.5	11.7
En. Loss per Turn (MeV)	0.72	1.68
τ_x (ms)	9.7	5.7
τ_y (ms)	18.1	7.8
τ_E (ms)	16.0	4.8

- scanning the fractional tune within $Q_x = 54$ to 55 and $Q_y = 20$ to 21 , maintaining the ‘-I’ and cell phase advance constraints;
- stepping the horizontal integer tune from 54.2 to 62.2 ;
- increasing the chromaticity in integer steps from $[+2, +2]$ to $[+10, +10]$ at fixed tune point;
- running MOGA optimisations with a variety of constraints and variable parameters.

Two alternative operating modes using the nominal lattice hardware were found during this study, one with reduced beta-functions at the IDs to improve the phase-space matching to the photon beams, the other with smaller natural emittance [4]. These have smaller dynamic aperture and lifetimes than the baseline lattice and are under consideration for a future ‘brightness’ upgrade.

Content from this work may be used under the terms of the CC BY 4.0 licence (© 2022). Any distribution of this work must maintain attribution to the author(s), title of the work, publisher, and DOI

Injection Scheme

The Diamond-II storage ring design includes hardware capable of supporting a variety of injection schemes. The majority of equipment is located in the first long straight section (I01), with four single-bunch stripline kickers located in the first mid-straight (K01). A schematic of I01 is given in Fig. 2. The straight contains the following: one thick (3 mm) and one thin (1 mm) septum magnet; four DC chicane magnets for adjusting the position and angle of the stored beam with respect to the injection septum; four 6 μ s half-sine dipole kickers for bumping the stored beam towards the septum plate.

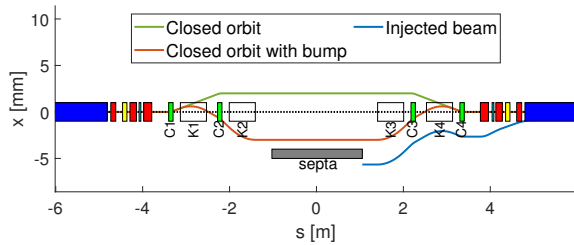


Figure 2: Injected and stored beam trajectories in I01 for late-stage commissioning and initial user operation.

The following injection stages are foreseen:

1. initial beam threading using the dipole kickers set for on-axis injection;
2. first accumulation using the dipole kickers set for aperture-sharing injection;
3. late-stage commissioning and initial user operation using the dipole kickers set for closed orbit bump;
4. transparent top-up injection using single-bunch stripline kickers set for aperture-sharing injection.

The single-bunch aperture sharing injection scheme shown in Fig. 3 has been adopted for top-up in user time due to its superior transparency compared with the standard four-kicker bump [5]. Assuming pulse durations below 3 ns, only 1 out of 899 stored bunches will be perturbed by the striplines during injection, thereby keeping the photon beam intensity stable to 0.1 %. As such, the largest perturbations are anticipated to come from septum leakage fields. Studies of aperture-sharing injection have also demonstrated the process is robust to realistic steering and focussing errors in the transfer line as well as to pulsed magnet jitter.

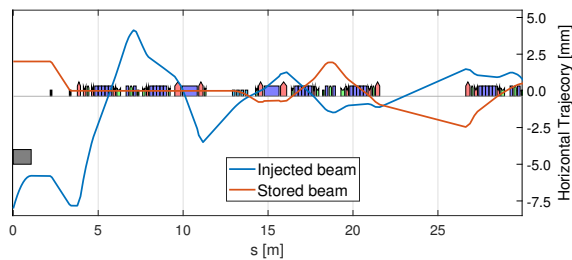


Figure 3: Trajectory of stored and injected bunches during aperture sharing injection. The striplines are at $s = 13$ m.

Optics Perturbations

The ability to commission and operate the storage ring in the presence of field and alignment errors has been cross-checked using the Simulated Commissioning Toolbox [6]. The planned correction procedures were able to restore the design optics to the percent-level and to recover the lifetime and dynamic aperture to close to the ideal values.

A significant source of error comes from the cross-talk between the magnetic fields. For Diamond-II, the minimum magnet separation was set to 75 mm for the hard-edge model. The resulting cross-talk was studied by inserting thin-lens elements between the magnets and setting the integrated multipole components according to OPERA models of the combined elements. Without correction, the cross talk was found to cause orbit distortions of ~ 0.7 mm and a vertical tune-shift of almost 1 unit. However, this can be almost fully corrected by simply adjusting the nominal magnet setpoints and B-fields to anticipate the cross-talk.

One final source of optics perturbation comes from the insertion devices (IDs). The existing storage ring contains 28 IDs, the majority of which will be retained or upgraded for Diamond-II. In addition, a number of new beamlines will be installed in the mid-straight and in straight I17. To compensate the perturbations due to these IDs a combination of a static LOCO correction, active shim wires on the APPLE-II IDs and a tune feedback is foreseen [7].

Collective Effects

An impedance database has been constructed for the Diamond-II vacuum chambers including both resistive-wall and geometric components. The resistive wall contributions have been calculated using ImpedanceWake2D [8] (including NEG coatings) and the geometric contributions modelled using CST [9]. This data was normalised with the local β -function and combined in a single impedance element to be used in the one-turn-map tracking model [10].

Single-bunch instability thresholds were determined for a variety of conditions, with good agreement found between tracking studies and analytical predictions [11]. In the longitudinal plane, the microwave instability threshold was 2 mA with IDs open increasing to 2.5 mA for IDs closed, compared to the nominal bunch currents of 0.3 mA in standard mode and 1.6 mA in hybrid. In the transverse plane, a minimum chromaticity of $[+1, +1]$ is required to achieve the hybrid bunch current. Studies of coupled-bunch instabilities are ongoing. Early results using purely resistive-wall impedance in the transverse and main cavity higher-order modes in the longitudinal indicate additional measures such as a bunch-by-bunch feedback will be required if the target 300 mA in standard mode is to be achieved [12].

A passive super-conducting harmonic cavity will be installed, similar to the ones in use at Elettra and SLS [13, 14]. Inclusion of this cavity will have a number of benefits, including increasing the Touschek lifetime, raising the instability thresholds described above and reducing in the impact of intra-beam scattering (see Fig. 4).

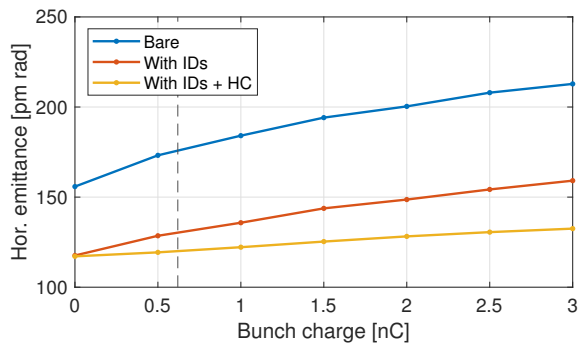


Figure 4: Impact of IBS on the horizontal emittance including longitudinal impedance ($\epsilon_y = 8$ pm.rad). The bunch charge in standard mode is highlighted.

FINAL PERFORMANCE ESTIMATES

To compute the expected beam lifetime in standard mode (300 mA, 899 bunches, $\epsilon_y = 8$ pm.rad), the results from simulated commissioning have been used to calculate the expected dynamic and momentum aperture over 40 seeds. These are shown in Fig. 5, for which the collimator apertures are found to dominate. The bunch-dependent Touschek lifetime can be calculated from the momentum acceptance, including the impact of IBS, longitudinal broadband impedance, IDs, harmonic cavity and physical apertures (see Fig. 6). The gas lifetime as a function of conditioning dose is shown in Fig. 7. This has been computed using the s-dependent pressure profile for both saturated and unsaturated NEG coating. A summary of the equilibrium beam parameters is given in Table 2. The gas lifetimes are quoted for 100 Ah conditioning time and unsaturated NEG.

Table 2: Equilibrium Beam Parameters in Standard Mode and Average Lifetime Components over 40 Seeds

Parameter	Bare Lattice	IDs Closed
Horizontal Emittance	163 pm.rad	120.0 pm.rad
Energy Spread	0.095 %	0.109 %
Bunch Length	49.1 ps	48.1 ps
Touschek (without HC)	2.8 ± 0.1 h	2.8 ± 0.1 h
Touschek (with HC)	8.2 ± 0.3 h	8.8 ± 0.5 h
Coulomb	60.0 ± 7.2 h	59.7 ± 7.4 h
Bremsstrahlung	277.5 ± 0.5 h	276.6 ± 0.7 h
Total (without HC)	2.6 ± 0.1 h	2.6 ± 0.1 h
Total (with HC)	7.0 ± 0.2 h	7.5 ± 0.4 h

FUTURE STUDIES

Further work is planned to refine and update the impedance model as the engineering work progresses, alongside updates to the error-model and cross-talk effects used during simulated commissioning. Further improvements to the nonlinear lattice is also desirable, either through numerical optimisation or via re-configuring the sextupole families.

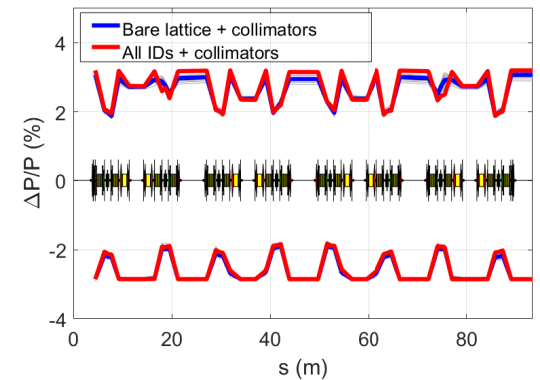
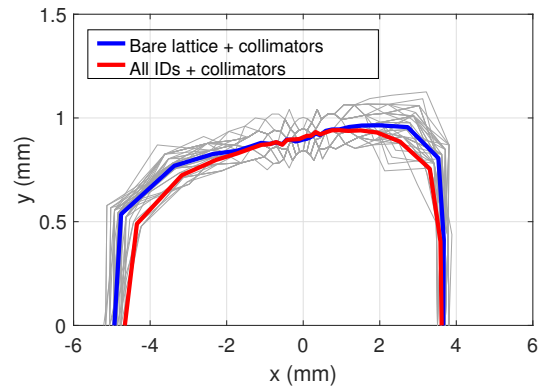


Figure 5: Average dynamic (top) and momentum (bottom) apertures after simulated commissioning.

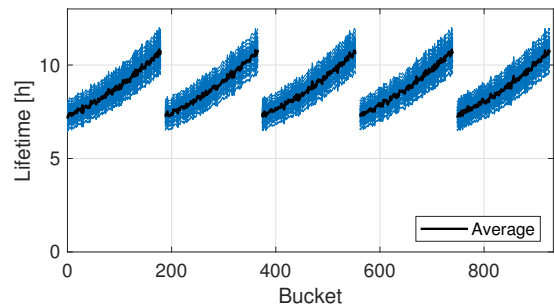


Figure 6: Bunch-dependent Touschek lifetime (standard mode, with IDs).

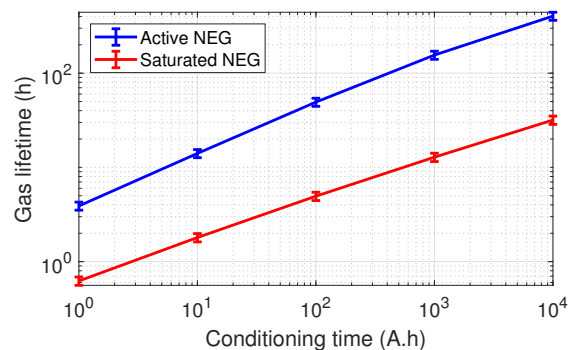


Figure 7: Gas Lifetime as a function of conditioning dose.

REFERENCES

- [1] H. Ghasem, I. P. S. Martin, and B. Singh, “Progress with the Diamond-II Storage Ring Lattice”, in *Proc. IPAC’21*, Campinas, Brazil, May 2021, pp. 3973–3976. doi:10.18429/JACoW-IPAC2021-THPAB090
- [2] “Diamond-II Technical Design Report”, Diamond Light Source, to be published, <https://www.diamond.ac.uk/Home/About/Vision/Diamond-II.html/>.
- [3] H. Ghasem, J. Kallestrup, I.P.S. Martin, “Collimation Studies for the Diamond-II Storage Ring”, presented at the IPAC’22, Bangkok, Thailand, June 2022, paper TUPOMS032, this conference.
- [4] H. Ghasem, I.P.S. Martin, B. Singh, “Tunability and Alternative Optics for the Diamond-II Storage Ring Upgrade”, presented at the IPAC’22, Bangkok, Thailand, June 2022, paper TUPOMS034, this conference.
- [5] J. Kallestrup, H. Ghasem, I.P.S. Martin, “Aperture Sharing Injection for Diamond-II”, presented at the IPAC’22, Bangkok, Thailand, June 2022, paper THPOPT018, this conference.
- [6] H.-C. Chao, R.T. Fielder, J. Kallestrup, I.P.S. Martin, B. Singh, “Commissioning Simulations for the Diamond-II Upgrade”, presented at the IPAC’22, Bangkok, Thailand, June 2022, paper THPOPT016, this conference.
- [7] B. Singh, R.T. Fielder, H. Ghasem, J. Kallestrup, I.P.S. Martin, T. Olsson, “Impact of Insertion Devices on the Diamond-II Lattice”, presented at the IPAC’22, Bangkok, Thailand, June 2022, paper MOPOTK037, this conference.
- [8] <https://twiki.cern.ch/twiki/bin/view/ABPComputing/ImpedanceWake2/>.
- [9] CST Studio Suite, <https://www.3ds.com/products-services/simulia/products/cst-studio-suite/>.
- [10] M. Borland, “elegant: A Flexible SDDS-Compliant Code for Accelerator Simulation”, Advanced Photon Source LS-287, September 2000.
- [11] R.T. Fielder, H.-C. Chao, S. Wang, “Single Bunch Instability Studies with a New Impedance Lattice for Diamond-II”, presented at the IPAC’22, Bangkok, Thailand, June 2022, paper WEPOMS010, this conference.
- [12] S. Wang, H.-C. Chao, R.T. Fielder, T. Olsson, “Studies of Resistive Wall and HOM Coupled-Bunch Instabilities for Diamond-II”, presented at the IPAC’22, Bangkok, Thailand, June 2022, paper WEPOMS010, this conference.
- [13] M. Pedrozzi *et al.*, “SLS Operational Performance with Third Harmonic Superconducting System”, in *Proc. SRF’03*, Lübeck, Germany, Sep. 2003, paper MOP25, pp. 91–94.
- [14] T. Olsson, H.-C. Chao, “Fill Pattern for Reducing Transient Beam Loading and Ion-Trapping in the Diamond-II Storage Ring”, presented at the IPAC’22, Bangkok, Thailand, Jun. 2022, paper TUPOMS031, this conference.